PVP-Vol. 233

PRESSURE VESSEL FRACTURE, FATIGUE, AND LIFE MANAGEMENT

EDITED BY
S. BHANDARI
P. P. MILELLA
W. E. PENNELL

PVP-Vol. 233

PRESSURE VESSEL FRACTURE, FATIGUE, AND LIFE MANAGEMENT

presented at
THE 1992 PRESSURE VESSELS AND PIPING CONFERENCE
NEW ORLEANS, LOUISIANA
JUNE 21–25, 1992

sponsored by
THE PRESSURE VESSELS AND PIPING DIVISION, ASME

edited by
S. BHANDARI
FRAMATOME

P. P. MILELLA
ENEA/DISP.

W. E. PENNELL
OAK RIDGE NATIONAL LABORATORY

THE AMERICAN SOCIETY OF MECHANICAL ENGINEERS
345 East 47th Street ○ ○ United Engineering Center ○ ○ New York, N.Y. 10017

ISBN No. 0-7918-0774-6

Library of Congress
Catalog Number 92-53205

FOREWORD

This volume contains papers relating to the structural integrity assessment of pressure vessels and piping, with special emphasis on the effects of aging. The papers were prepared for technical sessions developed under the sponsorship of the ASME Pressure Vessels and Piping Division Committee for Design and Analysis. They were presented at the 1992 Pressure Vessels and Piping Division Conference in New Orleans, Louisiana, June 21–25.

The primary objective of the sponsoring organization is to provide a forum for the dissemination and discussion of information on development and application of technology for the structural integrity assessment of pressure vessels and piping. This publication includes contributions from authors from Czechoslovakia, Denmark, France, Germany, Italy, Japan, the United Kingdom, and the United States.

The papers are organized in five sections, each with a particular emphasis as indicated in the following section titles.

- Pressure Vessel Life Management
- Fracture Characterization Using Local and Dual-Parameter Approaches
- Stratification and Thermal Fatigue
- Creep, Fatigue, and Fracture
- Integrated Approach to Integrity Assessment of Pressure Components

Papers in this publication were subjected to the standard ASME peer-review process and the editors would like to thank the reviewers for their time and effort. In particular, the editors would like to thank the session chairmen who coordinated peer reviews for the papers in their sessions. The success of any technical conference depends on the individual efforts of the authors and the editors congratulate the authors for their outstanding work and thank them for their cooperation in putting the manuscripts together in a timely fashion. The editors would also like to acknowledge the support and encouragement provided by the sponsoring ASME Pressure Vessels and Piping Division Committee.

S. Bhandari
P. P. Milella
W. E. Pennell

CONTENTS

INTRODUCTION

PRESSURE VESSEL LIFE MANAGEMENT

K. Kussmaul, W. E. Pennell, and E. Smith

Aging degradation in pressure vessels is addressed in the design process by placing a service life limit on the vessels and including a comprehensive evaluation of all relevant aging mechanisms in the design support analysis. Recent developments, particularly in the nuclear power industry, have emphasized the need for research and development to further refine technology used to assess the structural integrity of aged pressure vessels. The need for this refinement reflects (a) the discovery that some aging processes are occurring at a rate higher than anticipated in the design process and (b) recognition of the considerable economic incentive for extending the service life of aged pressure vessels.

This section contains 12 papers addressing a range of aging mechanisms, aging evaluation procedures and aging control procedures for both nuclear and non-nuclear pressure vessels.

PVP-Vol. 233, Pressure Vessel Fracture, Fatigue,
and Life Management
ASME 1992

FATIGUE BEHAVIOR IN CLOSURES OF PRESSURIZED-WATER-REACTOR VESSELS

J. Vagner and F. Mermaz
Framatome
Saint Marcel, France

C. Rieg
Electricité de France Septen
Villeurbanne, France

ABSTRACT

The closures of P.W.R. vessels are subjected to important cyclic loading during the normal operating conditions. Their service life is justified using computational means which allow the evaluation of the stress fields and using fatigue curves issued from codes.

Fatigue tests have been realized with 1/4 scale models of closure studs. This similitude investigation permits to build a fatigue curve integrating the global behaviour of the reactor closures.

This paper presents the fatigue tests and the justification of the new experimental law. Different examples are given to illustrate the gain in terms of usage factor.

INTRODUCTION

The threaded assemblies constitute complex mechanical zones because they are statically indeterminate. The modelling of their mechanical behaviour was the subject of many computational analyses. They permit to improve the evaluation of the stress field in threaded parts of nominal [1] or non-conform [2] assemblies. Yet if the actual state of stress can be determined accurately the determination of fatigue behaviour is largely dependent on the knowledge of damage parameters.

Previous analyses [3] have shown the conservatism of the numerical analysis when compared to experimental low-cycle fatigue failure. A similitude experiment has been performed in accordance with the appendix ZII of the RCCM code [4] which permits to build a fatigue curve based on the tensile stress range in the shank of the stud. This will be used in the next analyses to evaluate the life time of reactor closures with respect to the crack initiation and to failure

METHOD

The experimental procedure proposed in the appendix ZII of the RCCM code defines the safety coefficients K_s and K_n to apply to the experimental points obtained with test models : K_s and K_n respectively apply to the stress level and the number of cycles. These coefficients integrate different effects of the similitude such as size effect(K_{s1}), surface finish (K_{sf}), temperature (K_{st}) and the number of replicate tests performed (K_{ss}) :

$$K_s = K_{s1} \times K_{sf} \times K_{st} \times K_{ss}$$

$$K_n = K_s^{4.3}$$

The similitude representation of the damage, the crack initiation and the crack propagation in thread root is difficult since many parameters intervene :

- the capacity of the test installation obliges to realize the geometry scaled to 1/4 : the diameter of the shank is 37.375 milimeters and the threaded parts are made at M38.375 x 1 (milimeters) (ISO) (figure 1). The geometrical similitude is more particularly respected for the engaged lengths, the thread root radius and the internal thread of the flange (with counter sinking). This parameters significantly intervene on the stress level which monitors the damage. Like the real studs, the test studs are machined. Some geometrical differences are induced by this machining, notably about the gaps, however their effects are more pessimistic with the test models than with the real studs ;
- the materials used for the models are the same as those employed in the industrial fabrication. Their mechanical caracteristics conform to the usual specification ; these materials are respectively :
  . for the studs : 40 NCD 7 3 (SA 540 B 24 cl. 3)
  (Sy = 980 MPa, Su = 1100 MPa)
  . for the vessel flanges : 16 MND 5 (A 533 B cl. 1)
  (Sy = 485 MPa, Su = 620 MPa)
- the test installation (figure 1) permits the cyclic loading of the stud. The efforts are applied at the top by a washer and a nut and at the bottom by a threaded insert representing the vessel flange. The stiffness of the latter is not correctly represented, but its influence is limited at the lower threads which are the least loaded parts. The spherical washers eliminate the bending loads.

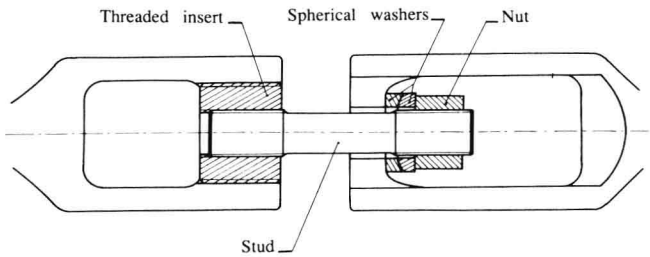

Fig. 1 : test installation

The damage depends highly on the geometry of the threads. This local effect is not correctly represented by a global parameter as the usual formulae (Neuber, Peterson, ASME III or RCCM) propose for smooth specimens.

To determine the size effect in this specific problem, different notch models are realized (figure 2) : two models ϕ 50 milimeters and two models ϕ 12.5 milimeters for each material. For the first models, the notch corresponds to a thread root of a real stud, for the latter, to a thread root in scale 1/4. These test results will permit to find a specific scaling factor (K_l).

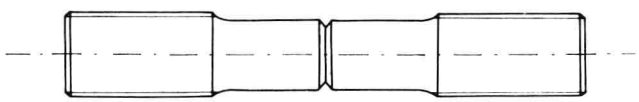

Fig. 2 : notch model

Accounting for the machining process, the factor for the effect of the surface finish is conservatively set to 1.

The tests are realized at room temperature (the temperature has no effect on the fatigue behaviour of assembly materials). Therefore, the factor K_{st} is equal to 1.

The factor for the statistical variation depends on the number of identical tests.

The parameters of this experimental analysis are the stress intensity in the shank of the stud and the number of cycles to initiation (or the number of cycles to failure). Each test gives an experimental point and two other points are determined by using the two coefficients K_s and K_n. The new fatigue curve is the envelope of these points.

EXPERIMENTAL PROGRAMME

The programme is performed with 12 identical models (nut, stud, insert). Four cyclic loadings are selected according to the loads existing in the vessel closure. The most severe loadings correspond to the opening/closing of the reactor vessel (10/500 MPa) and to the reactor heatup/cooldown (150/400 MPa). Two cyclic loads correspond to the normal operating conditions (250 to 400 MPa and 300 to 400 MPa). The cyclic loading is load controlled (with a constant range) and the alternating stress is corrected with the Peterson formula to account for the mean stress :

$$\sigma_{cor} = \frac{7\,\sigma_a}{8 - \left(1 + \frac{\sigma_m^*}{S_u}\right)^3}$$

where :

$\sigma_m^* = 0$ if $K_t \cdot \sigma_a > \sigma_{cy}$

$\sigma_m^* = \sigma_{cy} - K_t \cdot \sigma_a$ if $K_t \cdot (\sigma_a + \sigma_m) > \sigma_{cy}$

$\sigma_m^* = K_t \cdot \sigma_m$ if $K_t \cdot (\sigma_a + \sigma_m) < \sigma_{cy}$

and :

$\sigma_m = (\sigma_{max} + \sigma_{min})/2$

$\sigma_a = (\sigma_{max} - \sigma_{min})/2$

σ_a and σ_m are the stresses in the shank of the stud. K_t is the stress concentration factor which characterizes the threads (K_t = 4). The cyclic yield stress (σ_{cy} = 790 MPa) characterizing the bolting materials is determined from reference [5]. The Peterson's formula is furthermore validated for the materials used in this programme by the reference [6]. So the four cyclic loads are characterized by the corrected stress intensities : 245, 146, 105 and 80 MPa.

The notch models used to determine the size effect are cycled with the highest load (10 to 500 MPa).

The size effect is determined as follows :

- for each material, we determine the minimum number of cycles to initiation (and to failure) on full scale (N1) and on 1/4 scale models (N4),
- the size effect is the maximum value of N4/N1 between the intiation and the failure.

All the fatigue tests are realized at the same frequency : 4 Hz.

The initiation is detected by an acoustic emission detector and confirmed by a liquid penetrant examination. The minimal radial depth of detected defects measures between two and four milimeters.

RESULTS

Fracture always occurs in the stud at the level of the first thread. The results are relatively little dispersed (table 1) and show a good correlation between the two detection means.

Number of the stud	Number of the insert	Number of the nut	$\sigma_{min}/\sigma_{max}$ (MPa)	σ_{cor} MPa	Number of cycles to initiation	Number of cycles to failure
1	1	1	10/500	245		8500
2	2	2	10/500	245	10700	11800
10	5	10	10/500	245	7100	11400
12	12	12	10/500	245	6500	10400
5	5	5	150/400	146	24400	43200
6	6	6	150/400	146	30600	42900
4	4	4	250/400	105		102500
7	7	7	250/400	105	66500	180700
9	7	9	250/400	105	47300	264000
3	3	3	300/400	80		1000000
8	3	8	300/400	80	805000	941000
11	5	11	300/400	80	616000	748900

Table 1 – Models for fatigue tests at scale 1/4

The results moreover permit to affirm that the fatigue life of the threaded flange is twice as great as that of the stud. In fact, all the inserts which have been used twice or three times never failed before the new stud.

The results obtained with the notch models (table 2) show that the fatigue behaviour varies with the materials. A size effect appears for the stud material and not for the flange material. The high load perhaps hides this effect because of so very outspread plastic zones. Complementary tests will be performed to double the number of tests. The load of this next series will be smaller, it will permit the verification of the hypothesis about the flange material. This series will also permit to confirm or not the size factor retained :

$$K_t = \frac{4600}{2000} = 2.3$$

$$K_{\sigma 1} = (2,3)^{\frac{1}{4,3}} = 1,213$$

This value is close to those calculated with Neuber (1.11), Peterson (1.37), ASME III and RCCM (1.35) formulae . It is admitted for the two materials awaiting complementary experimental confirmation.

Material	Model	Number of cycles to initiation	Number of cycles to failure
SA 540 B 24	ϕ 12.5	5300	8973
		4600	8033
	ϕ 50	2000	6100
		3500	6900
16 MND 5	ϕ 12.5	3020	4933
		2800	5313
	ϕ 50	4500	7200
		3300	6200

Table 2 – Notch models to determine the effect of size (σ_{cor} = 245 MPa)

Two fatigue curves are proposed (figure 3), one for initiation, the other for failure. Compared to the reference curve (3 Sm) of codes (they are the same for the ASME III and RCCM), they display a gain increasing with the number of cycles.

The fatigue life of the threaded flange is taken conservatively twice that of the stud. Consequently, the usage factor is divided by two.

EXPERIMENTAL FATIGUE CURVES

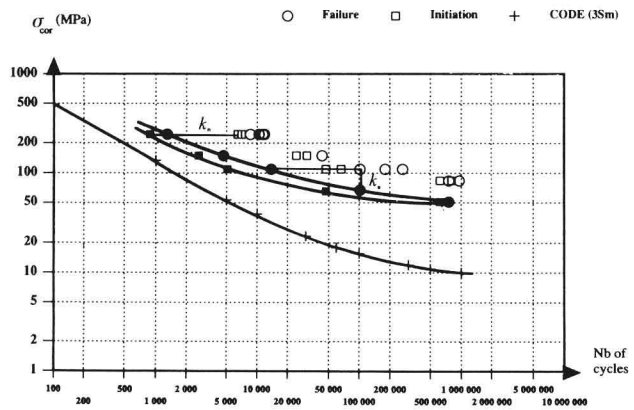

Fig. 3

INDUSTRIAL APPLICATIONS

The application of this experimental fatigue curve (that with crack initiation) to 900 and 1300 MWe French nuclear power plants has reduced stud usage factor to 50 % and thread flange usage factor to 25 % of the values previously obtained with RCCM curves.

The following two points must be noticed :

- the real fatigue lifetime of closures appears higher than that estimated with the design rules,
- the internal threaded parts are less sollicited than the stud. This leads to a situation somewhat different from what design rules predict and is favourable in maintenance problems.

CONCLUSION

This fatigue study performed in the framework of appendix ZII of RCCM code leads to a new experimental fatigue curve. It integrates the global behaviour of the closure assembly and permits the determination of the stud usage factor from the stress variation in the shank. The threaded parts usage factor is conservatively evaluated as half of that of the stud. The size effect will be confirmed by complementary tests with notch models.

The proposed method leads to important fatigue lifetime evaluation for 900 and 1300 MWe nuclear plants. The experimental nature of results excludes all excessive generalization. Its use permits in typical situations to avoid computational problems. It meets the objectives assigned.

ACKNOWLEDGMENTS

The authors wish to thank M. LAURAIN and his colleagues of the "Laboratoire du Service Technique des Constructions et Armes Navales" who performed the fatigue tests of this program.

REFERENCES

[1] *ANDRIEUX S., LEGER A.*
"A multiple scaling method for the computation of threaded structures".
SMIRT 10 transactions vol. (August 1989) Lausanne, Switzerland.

[2] *BARTHELET B., LEGER A., WADIER Y.*
"Closure of PWR pressure vessel analysis of repairs and anomalies in the threaded stud–flange assembly".
SMIRT 11 transactions vol. D (August 1991) Tokyo, Japan.

[3] *BOSSER M., VAGNER J.*
"Fatigue behavior of a bolted assembly. A comparison between numerical analysis and experimental analysis."
SMIRT 9 transactions vol. (August 1987) Lausanne, Switzerland

[4] *RCCM : design and construction rules for mechanical components of PWR nuclear islands, 1988 edition, AFCEN, Paris, distributed by AFNOR.*

[5] *F. SNOW and B. LANGER*
"Low–cycle Fatigue of Large–Diameter Bolts".
Journal of Engineering for Industry.
Transactions of the ASME (February 1967).

[6] *Criteria of the ASME Boiler and pressure vessel code for design by analysis in sections III and VIII division 2 – ASME 1969.*

PVP-Vol. 233, Pressure Vessel Fracture, Fatigue,
and Life Management
ASME 1992

CLEAVAGE FRACTURE OF SPECIMENS CONTAINING AN UNDERCLAD CRACK

D. Moinereau
Electricité de France
Service RNE
Moret sur Loing, France

G. Debruyne
Electricité de France
Service IMA
Clamart, France

M. Bethmont and G. Rousselier
Electricité de France
Service RNE
Moret sur Loing, France

ABSTRACT

EDF has started a large program including tests on large size specimens and mechanical analyses to evaluate different methods of fracture analysis used in the reactor pressure vessel integrity assessments. Several specimens made of the ferritic steel A508 cl 3 with stainless steel cladding, containing artificial defects, are loaded in four point bending. Tests are performed at low temperature to simulate radiation embrittlement and to obtain crack instability by cleavage fracture.
Two tests have been recently performed on specimens containing an underclad crack at a temperature of about -170°C. The crack instability is obtained in each case by cleavage fracture, without crack arrest.
Each test is interpreted using linear elastic analysis and elastic-plastic analysis by two-dimensional finite element computations. One of the tests is also analysed by three-dimensional finite element computations. The fractures are well predicted by the elastic analysis (including the plasticity corrections defined in the French RCC-M code) and by the elastic-plastic analysis. The stress intensity factor (K_{cp} or K_j) is in each case in the scatter band of the base metal toughness. The comparison between the two-dimensional analysis and the three-dimensional analysis shows that the first one is very conservative.
The results show also that the mechanical analyses are too conservative if the cladding is not taken into account.

1. INTRODUCTION

The French approach on the integrity assessment of PWR vessels requires the existence of large margins with respect of brittle fracture ; the margins have to be demonstrated for all kinds of defects which could occur during manufacturing and particularly during cladding process. Several types of analysis can be used to assess the mechanical integrity of the flawed structure : linear elastic fracture mechanics with plasticity corrections, elastic-plastic analysis (1),(2),(3).
A programme including experimental tests on large size-mock-ups and numerical simulation of tests has been started by EDF (4),(5). Its purpose is, by comparison between predictions of analyses and experimental results, to validate different methods of fracture analysis, to evaluate their conservatism and the effect of the stainless steel cladding. Two mechanical tests have been recently performed on mock-ups containing an underclad crack. This paper describes the tests and presents the mechanical analyses of each test.

2. DESCRIPTION OF THE TESTS

2.1 Mock-ups

Two mock-ups containing an underclad crack are submitted to mechanical tests. The geometry chosen to simulate the vessel is a four-point bend bar specimen shown schematically in figure 1.
The central part of each mock-up, in A508 Cl3 ferritic steel, is extracted from a vessel shell ring. This forging is produced from a hollow ingot. The specimens of approximately 120 mm thickness, 1700 mm length and 145 mm width are clad layered on top surface using an automatic submerged-arc welding process. After cladding, a stress relief heat treatment is applied at 600°C during 8 hours on each mock-up.
The two mock-ups contain an artificial underclad crack made before cladding by machining and fatigue :

- in DSR3 mock-up, the crack size is 13 mm deep and 40 mm wide. The cladding, with thickness about 4.5 mm, is applied in only one layer (309L stainless steel).

- in DD2 mock-up, the crack size is 4.5 mm deep and 48 mm wide. The cladding is applied in two layers : a first layer in 309L stainless steel and a second layer in 308L stainless steel. The cladding thickness is in this case about 6 mm.

2.2 Materials characterization

The mechanical analyses of tests require to characterize the stainless steel cladding, the base metal and the heat-affected zone (HAZ). This characterization includes chemical analyses, Charpy impact tests, tensile tests, crack-growth resistance and fracture toughness.

The chemical composition of the forging is given in table 1. The cleavage fracture toughness, measured on 20% side-grooved CTJ25 specimens (net thickness 20 mm), is given in figure 2.

2.3 Testing conditions

The specimens are loaded in four-point bending with a 1450 mm major span and 450 mm minor span, as shown in figure 1. The purpose of tests is to obtain crack instability in base metal by cleavage fracture. With this aim, the tests are performed at very low temperature (about -170°C) to obtain a cleavage fracture toughness of the base metal representative of the vessel material toughness at the end of life.
Before the mechanical test, the mock-up is cooled with liquid nitrogen. The temperature is uniform inside the specimen after the cooling. The mock-up is insulated to avoid significant reheating during the fracture test.
Data collected during the test are load, load-point displacement, strains and temperatures. Strains are measured with strain gauges placed on the clad surface and on the opposite surface. Temperatures are measured with thermocouples placed on the surface and inside the specimen.

3. EXPERIMENTAL RESULTS

3.1 DSR3 mock-up

The mock-up fracture is reached with a load of 695 kN at a temperature of about -170°C. No crack arrest occured during the test. The fracture surface is presented in figure 3. The surface aspect is typical of a cleavage fracture, at least in the upper part of the section.
The crack shape is semi-elliptical with 13 mm depth and 40 mm width. The cladding thickness is 4.5 mm.

3.2 DD2 mock-up

The mock-up fracture is reached with a load of 890 kN at the temperature of about -170°C. No crack arrest occured during the test. The fracture surface is presented in figure 4. The surface aspect is also typical of a cleavage fracture, at least in the upper part of the section.
The crack shape is semi-elliptical with 4.5 mm depth and 48 mm width. The cladding thickness is 6 mm.

4. INTERPRETATION OF DSR3 TEST

The DSR3 is interpreted with linear elastic analysis and elastic-plastic analysis. This interpretation includes two-dimensional and three-dimensional finite element computations. Residual stresses are not taken into account in these analyses but their effect is not important (4).

4.1 Two-dimensional analyses

4.1.1 Linear elastic analysis

The stress intensity factor (SIF) K_I is calculated by a two-dimensional elastic computation performed with the SYSTUS finite element program developped by FRAMATOME. The residual stresses are not taken into account in this analysis. After the computation of the SIF K_I, two corrections are applied to take into account plasticity at the crack tips and in the cladding, according to the approach proposed for the analysis of the French PWR vessels (1 to 3).
The SIF obtained after corrections is compared to the base metal toughness K_{Ic} determined on the CT specimens. The 2D mesh is presented in figure 5 (size of the elements at the crack tip in base metal : 0.200 mm).

4.1.2 Elastic-plastic analysis

The SIF K_J is deduced from the calculation of the J integral . The integral J is calculated on several paths. The calculation is performed at the test temperature and takes into account only the mechanical loading (without residual stresses).

4.1.3 Results

The main results of analyses are presented in table 2 and in figure 6. At the critical load (695 kN), the stress intensity factors K_{cp} (including the plasticity corrections) and K_J are much larger than the minimum value of the base metal toughness K_{IC} at the test temperature. The comparison between the elastic analysis and the elastic-plastic analysis shows that the first one is very conservative, due to the plasticity corrections of RCC-M code.

4.2 Three-dimensional analyses (6)

4.2.1 Modelization of the mock-up

The mesh used for the analyses is presented in figure 7. Only a quarter of the specimen is meshed because of the symmetries. The mesh is composed with 20-node bricks and 15-node wedges. It contains less than 800 elements and 3000 nodes.
The finite element program used for the calculations is PERMAS. The stress intensity factor is calculated along the crack front by the means of the energy release rate G (G is obtained by the theta method detailed in (7,8)). Residual stresses are not taken into account in those calculations.

4.2.2 Results

The evolution of the stress intensity factor along the crack front in the base metal is shown for three calculations (linear elastic K_I, non linear-elastic K_{NLE}, linear elastic without taking into account the cladding) in figure 8. In each case, the maximum value of the SIF is obtained in the lower part of the crack (Φ=90°). Those values (table 2, figure 6) are always in the scatter band of the base metal toughness K_{Ic}. We can also notice the favourable effect of the cladding on the SIF values (decrease).

4.3 Comparison between 2D and 3D analyses

Figure 6 allows to compare the 2D and 3D analyses. The latter is more accurate and gives reasonable values of the stress intensity factors with respect to experimental values.

5. INTERPRETATION OF DD2 TEST

5.1 Elastic and elastic-plastic analyses

The DD2 test is interpreted with linear elastic analysis and elastic-plastic analysis. This interpretation includes only two-dimensional finite element computations. The calculations are performed with the SYSTUS finite element program. The residual stresses are not taken into account but their effect is not important (4).
The mesh is presented in figure 9. The size of the elements at the crack tip in base metal is 0.200 mm.
The main results of these analyses are indicated in table 3 and in figure 10.

At the critical load (890 kN), the stress intensity factors K_{cp} (including the plasticity corrections) and K_J are in the scatter band of base metal toughness K_{1c}. Those two values are much larger than the minimum value of the toughness.
The comparison between the elastic analysis and the elastic-plastic analysis shows that the first one is very conservative (K_{cp} = 79 MPa$\sqrt{m}$ with α=1.56, K_J = 61 MPa$\sqrt{m}$). The plasticity corrections of RCC-M code, and more particularly the α coefficient, represent too large corrections (1 to 5).

5.2 Simplified analysis without taking into account the cladding

In this analysis, we assume that the crack is a semi-elliptical surface crack. The dimensions of this crack are estimated from an extrapolation of the actual underclad crack. In this case, the stress intensity factor along the crack front is derived from formulae proposed by NEWMAN-RAJU (9).
For the DD2 mock-up, the stress intensity factor is maximum at the deepest point of the crack. At the critical load, K_I= 93 MPa.$\sqrt{m}$.
Compared to previous analyses, we see that the cladding has a favourable effect by decreasing the value of the stress intensity factor at the crack tip in base metal (K_I= 93 MPa.$\sqrt{m}$ without cladding, K_{cp} = 79 MPa.$\sqrt{m}$ with cladding).

6. CONCLUSION

EDF is carrying out an experimental and numerical study in order to validate and evaluate the conservatism of different methods of brittle analysis which are used in the reactor pressure vessel integrity assessments.
Two tests have been performed on large size mock-ups containing an underclad crack. A cleavage fracture initiated in base metal has been obtained in both cases at a temperature of about -170°C.
The fractures of both mock-ups are conservatively predicted by an elastic analysis including plasticity corrections and by an elastic-plastic analysis. The stress intensity factors calculated at the critical load are always in the scatter band of base metal toughness.
In the case of a small underclad crack (DD2 mock-up), the comparison between the elastic analysis and the elastic-plastic analysis shows that the first one is more conservative. It is due to the fact that the α correction proposed in French RCC-M code is very important as soon as the plastic zone at the crack tip in the cladding reaches a notable proportion of the remaining ligament.
In the case of a deep underclad crack (DSR3 mock-up with a crack of 13 mm depth), the three-dimensional analyses are more accurate than the classical two-dimensional analyses.

An important conclusion for an underclad crack is that a mechanical analysis could be too much conservative if the cladding is not taken into account.

ACKNOWLEDGEMENT

The authors thank Mr FAIDY, Mr RIEG and Mrs CHURIER-BOSSENNEC from Electricité de France (SEPTEN) for their cooperation and support for this study.

REFERENCES

(1) RCC-M , January 1988 Edition
"Design and Construction rules for mechanical components of PWR nuclear islands - RCC-M - AFCEN France"

(2) A. PELLISSIER-TANON, J. GRANDEMANGE, B. HOUSSIN, C. BUCHALET
"French experience on the verification of pressurized water reactor vessels integrity", EPRI Research project 2975-2, 1989

(3) A. PELLISSIER-TANON, S. BHANDARI, J. VAGNER
"Practical methods for surface and sub-surface cracks in reactor pressure vessels", ASME PRESSURE VESSELS AND PIPING CONFERENCE, San Diego, 1991

(4) D. MOINEREAU, M. BETHMONT, G. CHAS, G. ROUSSELIER
"Cleavage fracture of plates with small underclad crack : experiments presentation and interpretation by fracture mechanics", ASME PRESSURE VESSELS AND PIPING CONFERENCE, San Diego, 1991

(5) M. BETHMONT, D. MOINEREAU, G. ROUSSELIER
"Cleavage fracture of large specimens containing an underclad crack", SMIRT 11, Tokyo, 1991

(6) G. DEBRUYNE, D. MOINEREAU
"Crack analysis of cladded mock-ups in the frame of brittle and ductile fracture", SMIRT 11, Tokyo, 1991

(7) Y. WADIER, O. MALAK
"The Theta method applied to the analysis of 3D elastic-plastic cracked bodies", SMIRT 10, Anaheim, 1989

(8) P. DESTUYNDER, M. DJAOUA
"Equivalence de l'intégrale de Rice et du taux de restitution d'énergie", Compte-rendu de l' Académie des Sciences, Paris, 1980

(9) J.C. NEWMAN, I.S. RAJU
"An empirical stress-intensity factor equation for the surface crack"- Engineering Fracture Mechanics - vol.15, n°1-2, pp 185-192, 1981

TABLE 1 - CHEMICAL COMPOSITION OF THE FERRITIC STEEL A508 CI3 (weight %)

	C	S	P	Mn	Si	Ni	Cr	Mo	V	Cu	Co	Al
RCCM specification	⩽ 0.22	⩽0.008	⩽ 0.008	1.15 1.60	0.10 0.30	0.50 0.80	⩽ 0.25	0.43 0.57	⩽ 0.01	⩽ 0.08	⩽ 0.03	⩽ 0.04
Inner surface	0.14	0.004	0.006	1.31	0.19	0.72	0.17	0.51	< 0.01	0.07	< 0.01	0.015
1/4 thickness	0.18	0.004	0.006	1.32	0.19	0.73	0.17	0.51	< 0.01	0.07	⩽ 0.01	0.016

TABLE 2 - INTERPRETATION OF DSR3 TEST

Analysis	K_I MPa.$\sqrt{m}$	Irwin correction	α correction	K_{cp} MPa.$\sqrt{m}$	K_J, K_{NLE} MPa.$\sqrt{m}$
2D elastic	60	1.08	1.6	104	
2D elastic-plastic					80
3D elastic	48				
3D non linear elastic					53

TABLE 3 - INTERPRETATION OF DD2 TEST

Analysis	K_I MPa.$\sqrt{m}$	Irwin correction	α correction	K_{cp} MPa.$\sqrt{m}$	K_J MPa.$\sqrt{m}$
2D elastic	46	51	1.56	79	
2D elastic-plastic					61
3D simplified (surface crack)	93				